Phase diagrams and magnetic behavior of films with amorphization and anisotropy in surfaces

M. Bengrine, A. Benyoussef*, A. El Kenz, M. Loulidi and F. Mhirech.
Laboratoire de Magnétisme et de Physique des Hautes Energies, Département de Physique, Faculté des Sciences, Rabat, Maroc.

The phase diagrams and magnetic behavior of thin films with two amorphous surfaces, are investigated by the use of the effective field theory with correlations. The transition temperature dependence of the exchange integral at surfaces, coupling between surface and nearest-layers, film thickness, and structural fluctuations are studied. Some interesting phenomena can occur as wetting phenomena and compensation point.

PACS number(s): 75.70.Ak, 75.50.Kj

I. INTRODUCTION

In recent years, magnetic thin films have gained increasing interest for fundamental research and technological applications, in particular the effects of the surface and size on the phase transition.

Furthermore, the development of the molecular-beam-epitaxy technique and its application to the growth of thin metallic films has stimulated renewed interest in both experimental and theoretical thin-film magnetism. Experimentally, several reports have recently been published [1-4] on the structural and magnetic properties of multilayer such as Fe/Ni, where Fe layers may crystalise in a fcc or bcc structure depending on their thickness.

The disordered structure of amorphous ferromagnets must give rise to randomness in the interactions of the magnetic moments. These random interactions can be of two kinds: random isotropic exchange and random anisotropy. From the experimental point of view, the formation of disordered surface is usually considered to happen. Nevertheless, the research of surface magnetism with a disordered surface seems to be far from complete, although some progress has been noted [5-7]. Kaneyoshi and Jascur have studied the effects of surface anisotropy on the surface phase transition [8] where they discussed the magnetic behavior associated with the surface dilution as well as the surface single -ion anisotropy. Also, a surface amorphization has been studied [9,10].

The magnetic properties of an infinite Ising-type amorphized structures have been investigated [11,12] when the effect of amorphization on transition temperature has been studied. One of the more interesting problems to investigate in a magnetic system is the critical temperature when the system becomes finite and thus it loses symmetry in the direction perpendicular to the surface. Along with the development of new types of magnetic materials, studies on the properties of magnetic films have received much attention. It was found by Ferchmin and Maciejewski [13] that surface enrichment of an internally dilute Ising film is a possible source of surface magnetism.

Many approaches have been employed recently in investigating the magnetic behaviors of the model thin film system, e.g., the renormalization-group method, the finite-size scaling method [14].

In this paper we examine the effect of the amorphous surfaces, the amorphized coupling between surfaces and bulk and the size of the film on the critical behavior of Ising films, using the effective-field theory which is superior to the standard mean field theory. Due to the finite size, we expect that the film transition temperature may be different from the bulk one, more precisely, the transition temperature in the system is higher that the bulk and decreases with increasing film thickness. The proposed model also may have some concordance with other theoretical works [15] where the authors examined a ferromagnetic film with two disordered surfaces in which the disorder is represented by the concentration p of magnetic atoms at the surface.

This paper is a review of studies published in references 16, 17 and 18. The outline of this paper is as follows. In section II, we define the model and the method of effective field theory by the use of the differential operator technique [19,20]. In section III, we analyze the phase diagrams and the magnetic properties of the system. The section III.A is a study of a spin -1/2 Ising film [16]. The section III.B is reserved to a study of bulk with spin-1/2 limited by two surfaces with spin-1 [17], while the section III.C include some interesting phase diagrams concerning a bulk with spin-3/2, limited by two surfaces with spin-5/2 [18]. The section IV is reserved to our conclusions.

II. FORMULATION

We consider a ferromagnetic film with a simple cubic structure. Both the couplings $\overline{J_S}$ at the surface and the couplings $\overline{J_1}$ between the surface and the nearest-neighbor layer are different from those J inside the film (as shown in Fig. 1). The Hamiltonian of the system is given by:

$$H = -\sum_{ij} \overline{J_S}\mu_i\mu_j - J\sum_{mn} S_m S_n - \sum_{im} \overline{J_1}\mu_i S_m - D_1 \sum_i \mu_i^2 - D_2 \sum_m S_m^2 \qquad (1)$$

where the summation is carried out only over nearest-neighbour pairs of spins. μ_i and S_m are the spin operators respectively at the surface and in the bulk. $\overline{J_S}$ and J are the exchange interactions between spins at the

* e-mail: benvous@fsr.ac.ma

surface and in the bulk, respectively. The exchange interaction between each surface and the first layer is given by $\overline{J_1}$. D_1 and D_2 are the crystal-field interactions constant, respectively at the surfaces and in the bulk. $D_1 = D_2 = 0$ in the case of Ising-1/2 film. $D_1 = D$, in the case of spin-1 at the surfaces. $\overline{J_S}$ and $\overline{J_1}$ are assumed to be randomly distributed according to the Kaneyoshi distribution for amorphous magnets [20], namely,

$$P(\overline{J_k}) = \frac{1}{2}[\,\delta(\overline{J_k} - J_k - \Delta J_k) + \delta(\overline{J_k} - J_k + \Delta J_k)], \quad k = 1, S \tag{2}$$

The number of layers in the film with two disordered surfaces is equal to *N*. The two surfaces (layers *i=1, N*) have spin-1/2 (section III.A), spin-1 (section III.B) or spin 5/2 (section III.C), while the layers $2 \le i \le N-1$ have spin-1/2 (sections 3.1 and 3.2), $2 \le i \le N-1$ have spin -3/2 (section 3.3),. The problem is now the evaluation of the expectations values $< \mu_i >$ and $< S_m >$ for several values of the film size. The starting point for the statistics of our spin system is the exact-Callen identity [21].

For the first layer,

$$< \mu_i^z > = < e^{E_i \nabla} > f_1(x)\big|_{x=0} \tag{3}$$

with

$$E_i = \sum_{\delta} \overline{J_S} \mu^z_{i+\delta} + \sum_{\delta'} \overline{J_1} S^z_{i+\delta'} \tag{4}$$

$$f_1(x) = \frac{1}{2}\tanh(\frac{1}{2}\beta x), \text{ for } S = 1/2 \tag{5a}$$

$$f_1(x) = \frac{2\sinh(\beta x)}{2\cosh(\beta x) + \exp(-\beta D)}, \text{ for } S = 1 \tag{5b}$$

and for S= 5/2

$$f_1(x) = \frac{1}{2}\frac{5\sinh(\frac{5}{2}\beta x) + 3\sinh(\frac{3}{2}\beta x)\exp(-4\beta D_1) + \sinh(\frac{1}{2}\beta x)\exp(-6\beta D_1)}{\cosh(\frac{5}{2}\beta x) + \cosh(\frac{3}{2}\beta x)\exp(-4\beta D_1) + \cosh(\frac{1}{2}\beta x)\exp(-6\beta D_1)} \tag{5c}$$

For the second layer,

$$< S_m^z > = < e^{E_m \nabla} > f_2(x)\big|_{x=0} \tag{6}$$

with

$$E_m = J \sum_{\delta} S^z_{m+\delta} + \sum_{\delta'} \overline{J_1} \mu^z_{i+\delta'} + J \sum_{\delta''} S^z_{m+\delta''} \tag{7}$$

and

$$f_2(x) = \frac{1}{2}\tanh(\frac{1}{2}\beta x), \text{ for } S = 1/2 \tag{8a}$$

for S= 3/2

$$f_2(x) = \frac{1}{2}\frac{3\sinh(\frac{3}{2}\beta x) + \sinh(\frac{1}{2}\beta x)\exp(-2\beta D_2)}{\cosh(\frac{3}{2}\beta x) + \cosh(\frac{1}{2}\beta x)\exp(-2\beta D_2)} \tag{8b}$$

In the bulk

$$< S_n^z > = < e^{E_n \nabla} > f_2(x)\big|_{x=0} \tag{9}$$

with

$$E_n = J \sum_{\delta} S^z_{n+\delta} \tag{10}$$

Here $\beta = 1/K_B T$ and $\nabla = \partial/\partial x$ is a differential operator.

Using the differential operator technique and introducing the Van Der Waerden identity [22]:

For spin 1/2,

$$\exp(a\mu_i^z) = \cosh(\frac{1}{2}a) + 2\mu_i^z \sinh(\frac{1}{2}a) \tag{11}$$

$$\exp(aS_m^z) = \cosh(\frac{1}{2}a) + 2S_m^z \sinh(\frac{1}{2}a) \tag{12}$$

For spin 1

$$\exp(a\mu_i^z) = q\cosh(\frac{1}{2}a) + \mu_i^z \sinh(\frac{1}{2}a) + 1 - q, \tag{13}$$

where

$$q = < (\mu_i^z)^2 > \tag{14}$$

For spin >1,

$$\exp(a\mu_i^z) = \cosh(a\eta_1/\alpha) + \frac{\alpha}{\eta_1}\mu_i^z \sinh(a\eta_1/\alpha) \tag{15}$$

$$\exp(aS_m^z) = \cosh(a\eta_2/\alpha) + \frac{\alpha}{\eta_2} S_m^z \sinh(a\eta_2/\alpha) \tag{16}$$

where the parameters η_1 and η_2 are defined by:

$$\left(\frac{\eta_1}{\alpha}\right)^2 = <(\mu_i^z)^2> \quad (17)$$

$$\left(\frac{\eta_2}{\alpha}\right)^2 = <(S_m^z)^2> \quad (18)$$

The parameter α in eqs. (17) and (18) for a half-integer spin is $\alpha = 2$ and $\alpha = 1$ in the case of integer spin.

In the case of spin-1/2 Ising film, we have for each monolayer:

$$m_1 = \left[< cosh\left(\nabla \overline{J_S}/2\right)>_r + 2m_1 < sinh\left(\nabla \overline{J_S}/2\right)>_r\right]^4 \times \left[< cosh\left(\nabla \overline{J_1}/2\right)>_r + 2m_2 < sinh\left(\nabla \overline{J_1}/2\right)>_r\right] f_1(x)\Big|_{x=0} \quad (19a)$$

$$m_2 = \left[cosh\left(\nabla J/2\right) + 2m_2\, sinh\left(\nabla J/2\right)\right]^4 \times \left[< cosh\left(\nabla \overline{J_1}/2\right)>_r + 2m_1 < sinh\left(\nabla \overline{J_1}/2\right)>_r\right] \times \left[cosh\left(\nabla J/2\right) + 2m_3\, sinh\left(\nabla J/2\right)\right] f_2(x)\Big|_{x=0} \quad (19b)$$

and for $3 \le j \le N-3$

$$m_j = \left[cosh\left(\nabla J/2\right) + 2m_j\, sinh\left(\nabla J/2\right)\right]^4 \times \left[cosh\left(\nabla J/2\right) + 2m_{j+1}\, sinh\left(\nabla J/2\right)\right] \times \left[cosh\left(\nabla J/2\right) + 2m_{j-1}\, sinh\left(\nabla J/2\right)\right] f_2(x)\Big|_{x=0} \quad (19c)$$

)

In the case of spin-1 at the surfaces of the film and spin-1/2 in the bulk, we have for each monolayer:

$$m_1 = \left[q_1 < cosh\left(\overline{J_S}\nabla\right)>_r + m_1 < sinh\left(\overline{J_S}\nabla\right)>_r + 1 - q_1\right]^4 \times \left[< cosh\left(\overline{J_1}\nabla/2\right)>_r + 2m_2 < sinh\left(\overline{J_1}\nabla/2\right)>_r\right] f_1(x)\Big|_{x=0} \quad (20a)$$

$$q_1 = \left[q_1 < cosh\left(\overline{J_S}\nabla\right)>_r + m_1 < sinh\left(\overline{J_S}\nabla\right)>_r + 1 - q_1\right]^4 \times \left[< cosh\left(\overline{J_1}\nabla/2\right)>_r + 2m_2 < sinh\left(\overline{J_1}\nabla/2\right)>_r\right] g_1(x)\Big|_{x=0} \quad (20b)$$

$$m_2 = \left[cosh\left(J\nabla/2\right) + 2m_2\, sinh\left(J\nabla/2\right)\right]^4 \times \left[q_1 < cosh\left(\overline{J_1}\nabla\right)>_r + m_1 < sinh\left(\overline{J_1}\nabla\right)>_r + 1 - q_1\right] \times \left[cosh\left(J\nabla/2\right) + 2m_3\, sinh\left(J\nabla/2\right)\right] f_2(x)\Big|_{x=0} \quad (20c)$$

and for $3 \le j \le N-3$

$$m_j = \left[cosh\left(J\nabla/2\right) + 2m_j\, sinh\left(J\nabla/2\right)\right]^4 \times \left[cosh\left(J\nabla/2\right) + 2m_{j-1}\, sinh\left(J\nabla/2\right)\right] \times \left[cosh\left(J\nabla/2\right) + 2m_{j+1}\, sinh\left(J\nabla/2\right)\right] f_2(x)\Big|_{x=0} \quad (20d)$$

In the case of spin-5/2 at the surfaces of the film and spin-3/2 in the bulk, we have for each monolayer:

$$m_1 = \left[< cosh\left(\nabla \overline{J_S}\eta_1/2\right)>_r + \frac{2}{\eta_1} m_1 < sinh\left(\nabla \overline{J_S}\eta_1/2\right)>_r\right]^4 \times \left[< cosh\left(\nabla \overline{J_1}\eta_2/2\right)>_r + \frac{2}{\eta_2} m_2 < sinh\left(\nabla \overline{J_1}\eta_2/2\right)>_r\right] f_1(x)\Big|_{x=0} \quad (21a)$$

$$q_1 = \left[< cosh\left(\nabla \overline{J_S}\eta_1/2\right)>_r + \frac{2}{\eta_1} m_1 < sinh\left(\nabla \overline{J_S}\eta_1/2\right)>_r\right]^4 \times \left[< cosh\left(\nabla \overline{J_1}\eta_2/2\right)>_r + \frac{2}{\eta_2} m_2 < sinh\left(\nabla \overline{J_1}\eta_2/2\right)>_r\right] g_1(x)\Big|_{x=0} \quad (21b)$$

$$m_2 = \left[\cosh(\nabla J \eta_2 / 2) + \frac{2}{\eta_2} m_2 \sinh(\nabla J \eta_2 / 2) \right]^4 \times \left[< \cosh(\nabla \overline{J_1} \eta_1 / 2) >_r + \frac{2}{\eta_1} m_1 < \sinh(\nabla \overline{J_1} \eta_1 / 2) >_r \right] \times \left[\cosh(\nabla J \eta_2 / 2) + \frac{2}{\eta_2} m_3 \sinh(\nabla J \eta_2 / 2) \right] f_2(x) \Big|_{x=0} \quad (21c)$$

$$q_2 = \left[\cosh(\nabla J \eta_2 / 2) + \frac{2}{\eta_2} m_2 \sinh(\nabla J \eta_2 / 2) \right]^4 \times \left[< \cosh(\nabla \overline{J_1} \eta_1 / 2) >_r + \frac{2}{\eta_1} m_1 < \sinh(\nabla \overline{J_1} \eta_1 / 2) >_r \right] \times \left[\cosh(\nabla J \eta_2 / 2) + \frac{2}{\eta_2} m_3 \sinh(\nabla J \eta_2 / 2) \right] g_2(x) \Big|_{x=0} \quad (21d)$$

and for $3 \le j \le N - 2$

$$m_j = \left[\cosh(\nabla J \eta_2 / 2) + \frac{2}{\eta_2} m_j \sinh(\nabla J \eta_2 / 2) \right]^4 \times \left[< \cosh(\nabla \overline{J_1} \eta_1 / 2) >_r + \frac{2}{\eta_1} m_{j+1} < \sinh(\nabla \overline{J_1} \eta_1 / 2) >_r \right] \times \left[\cosh(\nabla J \eta_2 / 2) + \frac{2}{\eta_2} m_{j-1} \sinh(\nabla J \eta_2 / 2) \right] f_2(x) \Big|_{x=0} \quad (21e)$$

$$q_j = \left[\cosh(\nabla J \eta_2 / 2) + \frac{2}{\eta_2} m_j \sinh(\nabla J \eta_2 / 2) \right]^4 \times \left[< \cosh(\nabla \overline{J_1} \eta_1 / 2) >_r + \frac{2}{\eta_1} m_{j+1} < \sinh(\nabla \overline{J_1} \eta_1 / 2) >_r \right] \times \left[\cosh(\nabla J \eta_2 / 2) + \frac{2}{\eta_2} m_{j-1} \sinh(\nabla J \eta_2 / 2) \right] g_2(x) \Big|_{x=0} \quad (21f)$$

the functions $g_1(x)$ and $g_2(x)$ are given by

$$g_1(x) = \frac{2\cosh(\beta x)}{2\cosh(\beta x) + \exp(-\beta D)}, \text{ for } S = 1 \quad (22a)$$

for *S=5/2*

$$g_1(x) = \frac{1}{4} \frac{25\cosh\left|\frac{5}{2}\beta x\right| + 9\cosh\left(\frac{3}{2}\beta x\right)\exp(-4\beta D_1) + \cosh\left(\frac{1}{2}\beta x\right)\exp(-6\beta D_1)}{\cosh\left(\frac{5}{2}\beta x\right) + \cosh\left(\frac{3}{2}\beta x\right)\exp(-4\beta D_1) + \cosh\left(\frac{1}{2}\beta x\right)\exp(-6\beta D_1)} \quad (22b)$$

for *S= 3/2*

$$g_2(x) = \frac{1}{4} \frac{9\cosh(3\beta x/2) + 9\cosh(\beta x/2)\exp(-2\beta D_2)}{\cosh(3\beta x/2) + \cosh(\beta x/2)\exp(-2\beta D_2)} \quad (22c)$$

In the expression of m_j and q_j, the random bond averages are given by:

$$< \cosh(\nabla \overline{J_k}) >_r = \cosh(\nabla J_k \delta_k) \cosh(\nabla J_k) \quad (23)$$

$$< \sinh(\nabla \overline{J_k}) >= \cosh(\nabla J_k \delta_k) \sinh(\nabla J_k) \quad (24)$$

Expanding the right-hand sides of eqs. (19) to (21) we obtain the set of coupled equations. These coupled equations constitute the basis of the present work. We note that we will note write their expressions because of their complex forms. Moreover, these equations have been resolved numerically.

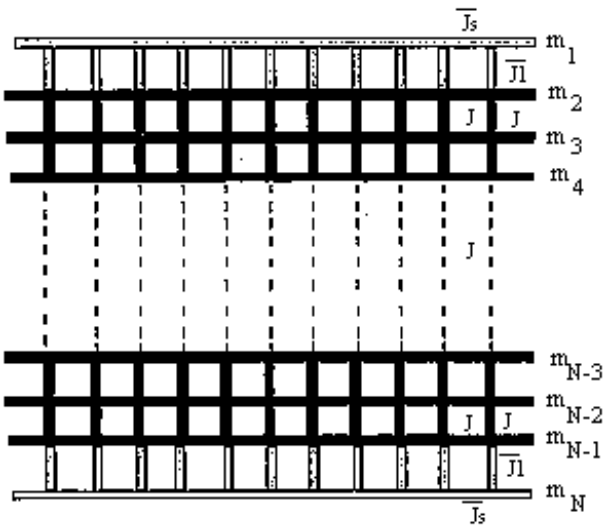

Fig. 1: Part of the two-dimensional cross-section through the simple cubic Ising lattice with amorphous surface. The full lines indicate the bulk exchange interaction J. Shaded lines indicate the exchange interactions $\overline{J}_S$ and $\overline{J}_1$.

III. PHASE DIAGRAMS AND MAGNETIC PROPERTIES

A. Spin 1/2 at the surfaces and in the bulk

To illustrate how the critical temperature varies with the coupling at the surfaces, we present in Fig. 2(a) our results for the amorphized case $\delta_S = 2$ and $\delta_1 = 0$. The phase transition from ferromagnetism to paramagnetism takes place when all the magnetizations

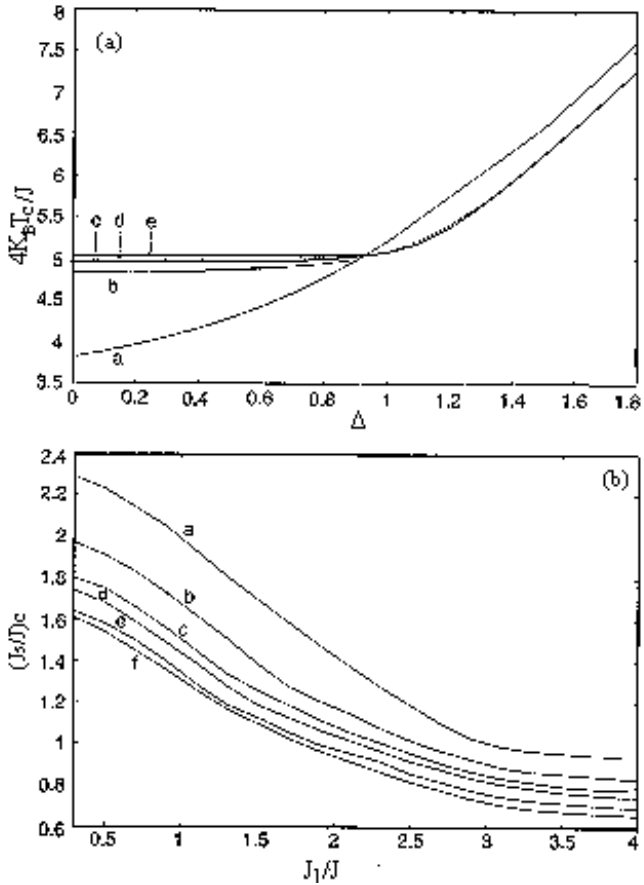

m_j of layers $1 \le j \le N$ vanish and not only the total magnetization of the film. We note that the phase diagram exhibits the same behavior as in the crystalline case ($\delta_S = \delta_1 = 0$). Indeed, when the exchange interactions at the surfaces are equal at those in the bulk, the transition temperature converge to the bulk transitions $4K_BT_c/J = 5.073$ with increasing film

Fig. 2: a) Phase diagrams in the space ($K_BT_c/J, \Delta$) for several values of film thickness N and for $J_1/J=1$, $\delta_S = 2$, $\delta_1 = 0$, $N=3$ (curve a), $N=7$ (curve b), 10 (curve c), 12 (curve d) and 16 (curve e). b) Phase diagrams in the space ($(J_S/J)_c, J_1/J$) for $N=16$, $\delta_1 = 0$. $\delta_S = 2$ (curve a), $\delta_S = 1.4$ (curve b), 1 (curve c), 0.8 (curve d), 0.4 (curve e) and 0 (curve f).

thickness N. Furthermore, the "special point" at which all the curves, for $N \ge 4$, are meet up, is given in the pure case by $\Delta_c = (J_S/J)_c - 1 = 0.307$; this value is given before in the semi-infinite system by the EFT [9,11]. On the other hand, this "special point" depends strongly on the amorphization. The corresponding phase diagram is shown in Fig. 2b. So the critical value $(J_S/J)_c$ as function of J_1/J, for $N=16$ and several values of δ_S is then plotted. As is seen, the critical value $(J_S/J)_c$ of coupling at the surface increases with increasing the surface amorphization δ_S. These results are in good agreement with diluted Ising films studied by J. C. Cressoni et al [22].

In Fig.3(a), the transition temperature is plotted as a function of the film size. $J_S/J=J_1/J$ is chosen, i.e., the couplings at the surface are equal to those between the surfaces and the nearest-neighbor in the first magnetic layer. So the transition temperature T_C may increase or decrease with N, according to the values of J_S/J, and converge at finite value. Example for $J_1/J=0.8$ (curve d) correspond to case that, when the number of layers N exceeds 15, the transition temperature approaches a bulk transition temperature ($4K_BT_c/J=5.073$) given by EFT. The case of large values of J_1/J can be explained by the fact that surface magnetism orders before the order of the bulk. If we increase the structure factor δ_1, (Fig. 3b), the critical temperature decreases and for any value of δ_1 we have the corresponding critical value of $(J_S/J)_C=(J_1/J)_C$ which give the bulk transition temperature. In fact, we recapitulate the situation: when the disorder between the surfaces and the bulk increases, the value of coupling $(J_S/J)_c=(J_1/J)_c$ corresponding to the bulk transition increases.

In order to study the magnetic properties of our system, it is necessary to solve the coupled equations (19a)-(19c). Therefore, we define the total magnetization M as

$$M = \frac{1}{N}\sum_{i=1}^{N} m_i \ . \qquad (25)$$

It is interesting to examine the case where the surface magnetization aligns antiparallel ($J_1/J<0$) to the magnetizmation in the bulk. Experimentally, it is reported that the coupling at the interface of Gd and Fe is antiferromagnetic [24,25].

In Fig. 4a we plot the magnetization M of the crystalline three layer film, as a function of the temperature for $J_S/J=0.5$. Various values of the ratio J_1/J are considered. As we can see, the magnetization M present a jump for a weak values of $|J_1/J|$ (curves a and b) owing to surfaces magnetizations. Indeed, if we decrease the temperature, and at critical value of T, the surfaces order. The corresponding magnetization m_1 starts by a negative value decreases ($|m_1|$ increases) up to temperature T_W where it presents a jump to positive value, this corresponds to wetting phenomenon [26].
In fact, at $T=T_W$ the bulk impose its order to surfaces. Moreover, a compensation temperature T^* appears between T_W and T_C ($T_W<T^*<T_C$). In this point, the total magnetization vanishes. This compensation point T^* also exists for $J_1/J=-1$ (curve c) while the wetting phenomenon disappears. However, in the case of strong coupling between the surface and the bulk (curve d) the magnetization at $T=0$ is negative one and increases to vanish. On the other hand, for the strong coupling at the surface (not presented) the magnetization is always positive at $T=0$, decreases and vanishes at a temperature higher than the bulk one. The wetting phenomenon is also present.

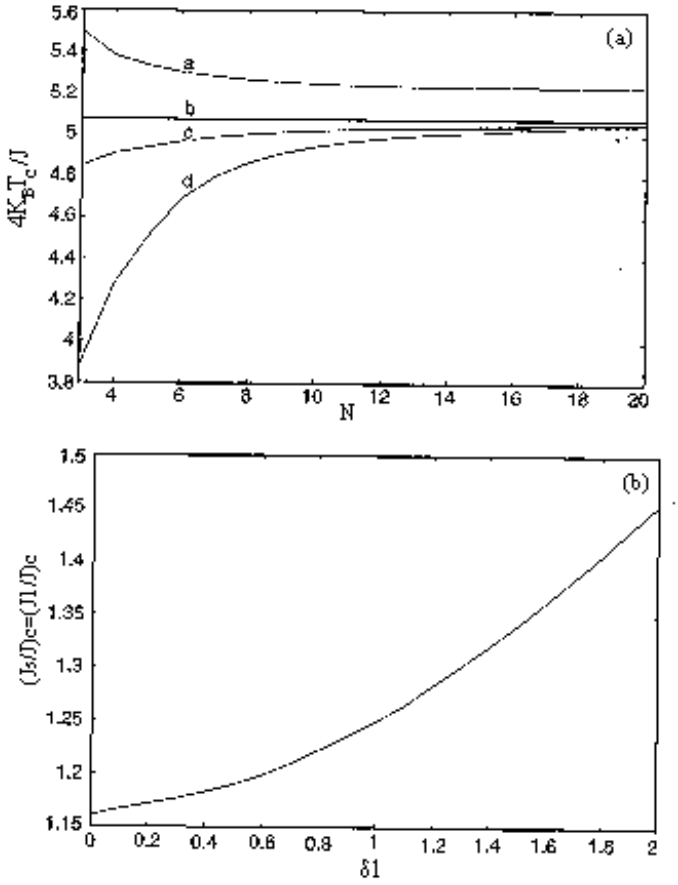

Fig. 3: a) The dependence of T_c on the film thickness N, $\delta_S = 0.2, \delta_1 = 1$. $J_1/J=J_S/J=1.4$ (curve a), 1.25 (curve b), 1.16 (curve c) and 0.8 (curve d).
b) Phase diagram in the space $(J_1/J=J_S/J, \delta_1)$ for $N=3$ and $\delta_S = 0.2$.

The effects of the amorphization on the three layer film is also investigated. Thus in Fig. 4b the magnetization M as a function of the temperature is plotted for $\delta_S = 2$ *and* $\delta_1 = 0.1$. In this figure we take $J_S/J=0.5$. The analogous phenomena have been found for the strong coupling at the surface. As is seen in Fig. 4b, the system don't exhibit a compensation point for the same value given in Fig. 4a. The wetting phenomenon is always present but for strong coupling J_1/J (curve d). For a weak value of J_1/J (curve a, b, c), the corresponding curves of M meet at a same point.

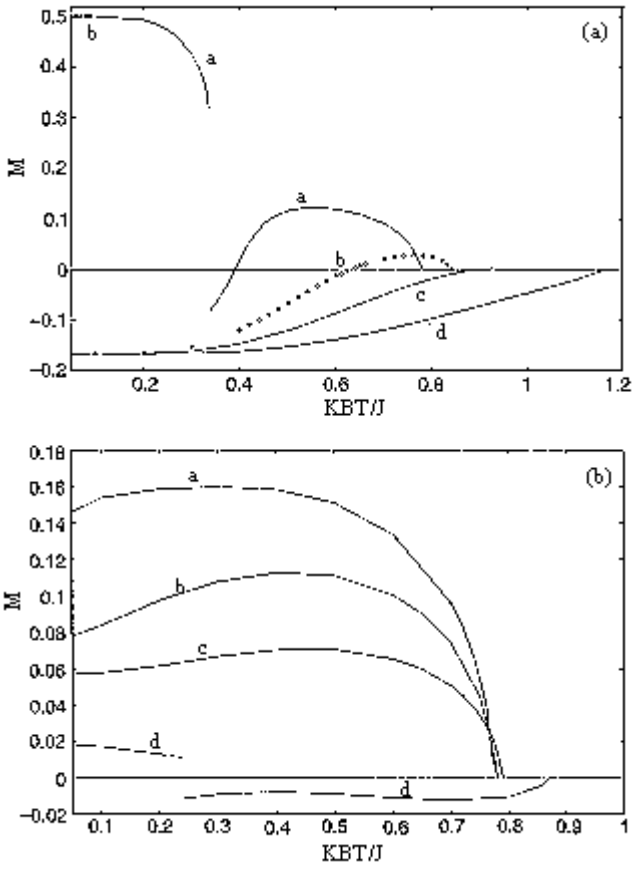

Fig. 4: The thermal variations of the total magnetization *M* for *Js/J=0.5* and *N=3*.

a) $\delta_S = \delta_1 = 0$, *J_1/J=-0.05* (curve a), *-0.5* (curve b), *-1* (curve c) and *-2* (curve d).

b) $\delta_S = 2, \delta_1 = 0$, *J_1/J=-0.05* (curve a), *-0.5* (curve b), *-1* (curve c) and *-2* (curve d).

B. Spin 1 at the surfaces and spin 1/2 in the bulk

Fig. 5 shows a typical phase diagram where the critical temperature T_C is a function of J_S/J for $J_1/J=0.1$ and $\delta_S = \delta_1 = 0.5$. In the figure, when the exchange interaction J_S is less than a «meeting point» $(J_S/J)^*$, the transition line para-ferro depends on the thickness of the film. As we increase the number of layers in the film, the transition temperature approaches the bulk one, i.e. $T_c/J=1.26$. on the contrary when J_S/J is greater than $(J_S/J)^*$, we have one alone transition line which is independent of the film thickness. If we increase the amorphization, qualitatively the behavior is the same as in the crystalline case, but the «meeting point» $(J_S/J)^*$ increases with amorphizations (δ_S and δ_1) in the system.

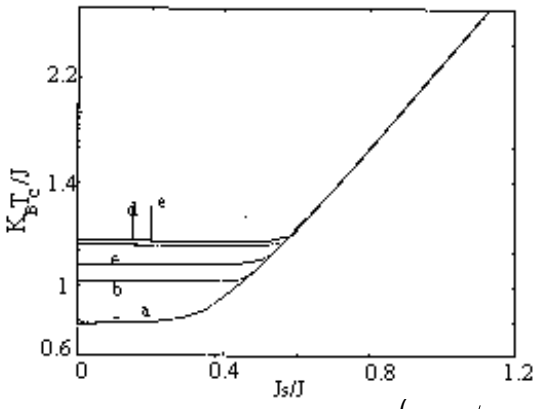

Fig. 5**:** The phase diagram in the space $(K_BT_c/J, J_S/J)$ for several values of film thickness *N* and for *D/J=0* and *J_1/J=0.1*, $\delta_S = \delta_1 = 0.5$, *N=3* (curve a), *N=4* (curve b), *N=5* (curve c), *N=10* (curve d) and *N=20* (curve e).

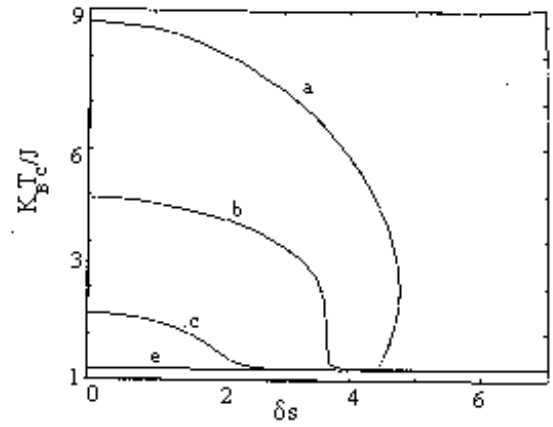

Fig. 6**:** The phase diagram in the space ($K_BT_c/J, \delta_S$) for *D/J=0, N=20,* $\delta_1 = 0$, *J_1/J=0.1, Js/J=4* (curve a), *Js/J=2* (curve b), *Js/J=1* (curve c), *Js/J=0.1* (curve d).

The small value of $(J_S/J)^*$ is then given in the crystalline case. Consequently, the paramagnetic region increases with amorphization. The analogous phenomenon occurs in (K_BT_c/J, J_1/J) plane.

In order to show the effect of surfaces amorphization in the film, the critical temperature T_c is plotted as a function of δ_S for *D/J*. Indeed, the case *N=20* with $\delta_1 = 0$, *J_1/J=0.1* is investigated for selected values of *J_S/J=4, 2, 1* and *0.1* (Fig. 6). We remark that at $\delta_S = 0$, the transition temperature increases with J_S. The same phenomenon occurs in the amorphized case $\delta_S \neq 0$.

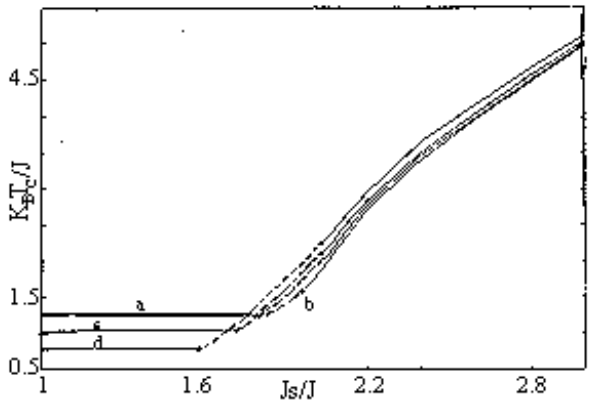

Fig. 7**:** The phase diagram in the space (K_BT_C/J,J_S/J) for *D/J=-4* and $J_1/J=1$. $\delta_S = \delta_1 = 0$, *N=20* (curve a), *N=10* (curve b), *N=4* (curve c) and *N=3* (curve d).

Only, the critical temperature decreases, with increasing δ_S , to the bulk transition temperature which corresponds to $J_S/J=0$. However, when the fluctuations δ_S and the exchange interaction J_S become strong enough, one can observe the appearance of the reentrant phenomena in the infinite systems. In fact the reentrant phenomenon can be observed for $J_S/J=4$ and $4.45 \le \delta_S \le 4.8$.

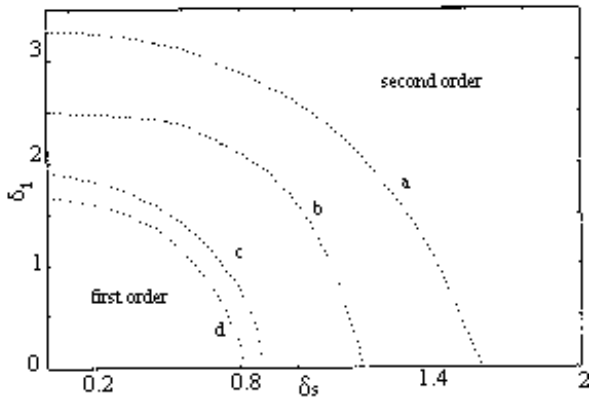

Fig. 8: The phase diagram in the space (δ_1 , δ_S) for *D/J=-4*, $J_S/J=1.9$ and $J_1/J=1$, *N=3* (curve a), *N=4* (curve b), *N=10* (curve c) and *N=20* (curve d).

Let us now clarify the effects of surface anisotropy on the phase diagram and critical value for surface ordering. Thus the value of crystal field is fixed at *D=-4*. In Fig 7 we show the phase diagram characterizing the state of the pure magnetic surface with $\delta_S = \delta_1 = 0$ and $J_1/J=1$. this figure expresses that the two critical points (open and black) exist for any value of the thickness of the film. However, by increasing the thickness the first-order phase transition line becomes small. Let us now increase the amorphization, we can remark that the first-order phase transition line decreases for each value of *N* in comparison with the others in Fig. 7. When we increase δ_S much more the first-order transition vanishes for any value of the thickness. This is due to the disorder at the surface. The Fig. 8 recapitulates the situation: δ_1 is plotted as a function of δ_S for $J_S/J=1.9$, $J_1/J=1$ and for several values of the thickness *N*. So we have a separation between the first order and second order regions. Furthermore, The first-order region decrease when *N* increases.

Multilayer films adsorbed on attractive substrates may exhibit variety of possible phase transitions, as has been reviewed by Pandit et al [27] and Ebner et al [28-31]. One type of transition is the layering transition, in which the thickness of a typical solid film increases discontinuously by one layer as the pressure is increased. Such transitions have been observed in a variety of systems including for example ^{4}He [32,33] and ethylene [34,35] adsorbed on graphite. The nth layering transition, from an (*n-1*) layer film to an nth layer film,

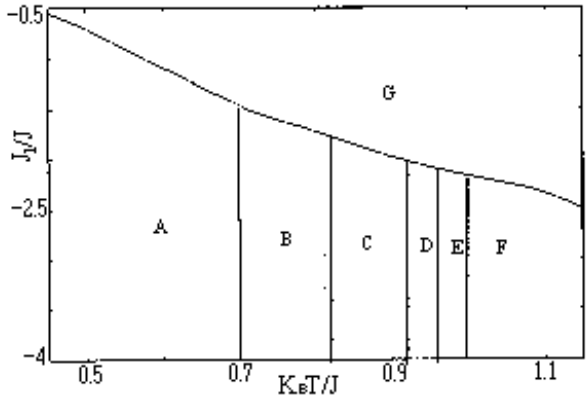

Fig. 9**:** The phase diagram in the space (J_1/J, K_BT/J) for *D/J=-4* and $J_S/J=1.5$ and $\delta_S = \delta_1 = 0$. The phases A, B, C, D, E, F and G represente respectively the following configurations (+-+ • • • • +-+), (+--+ • • • • +--+), (+---+ • • • • +---+), (+----+ • • • • +----+), (+-----+ • • • • +-----+), (+---- • • • • ----+) and (-+++ • • • • +++-).

is typically only present at low temperatures and may terminate as the temperature increases in a layering critical point $T_{c,n}$. The layering transition temperatures T_L are found for temperature below $T_{c,n}$. Such type of transitions has been extensively studied theoretically [36-41]. In Refs. [38] and [39] the authors are found that for sufficiently high temperature *T*, such that $T_L<T<T_{c,n}$, the number of layer transitions is equal to the number of layers in the film in both uniform and variable magnetization field cases. In the two last works [40,41], the authors give global phase diagrams which represent the connection between defect plane order and wetting phenomenon in the cases of crystallized [40] and amorphized [41] defect plane.

In the following, we will extend this work to study the wetting transition. We give a phase diagram which represent the wetting phenomenon in the case of crystalline thin film in which the coupling J_1 is taken as a negative value. So, the first layer (surface layer) is

coupled ferrimagnetically to the second layer (in the volume). In Fig. 9, the J_1/J versus T_c/J plots are depicted for $N=20$, $J_S/J=1.5$ and $D/J=-4$. As is shown in this figure, we can distinguish two different behaviors observed for $J_1/J<-2.5$ and $J_1/J\geq -2.5$. In the first case, the surface orders at a temperature higher than that of

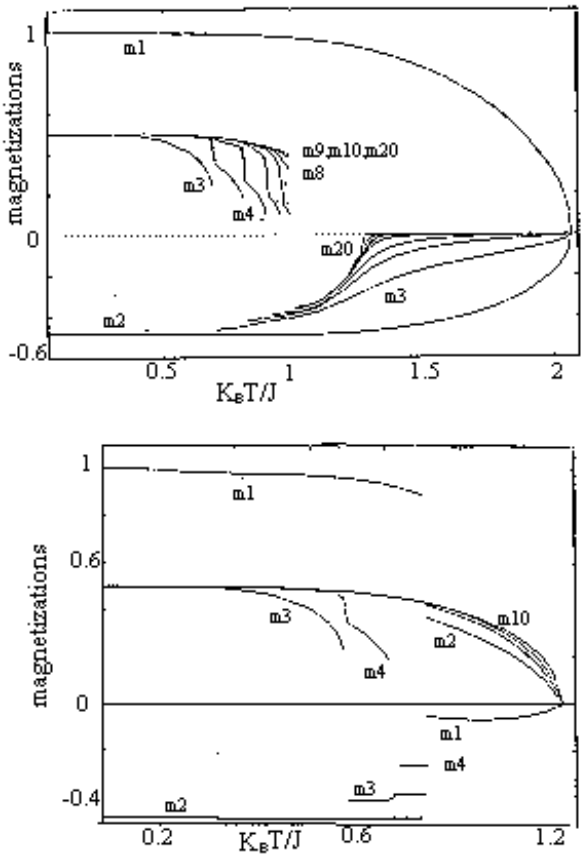

Fig. 10: The thermal variations of the magnetizations for $D/J=-4$, $\delta_S=\delta_1=0$, $J_S/J=1.5$ and $N=20$. (a) $J_1/J=-4$. (b) $J_1/J=-2$.

the bulk T_c^b. So, the layer transition occurs at temperature below T_c^b. The starting point, at $T=0^0K$, is given by the magnetizations $m_1>0$, $m_2<0$, $m_i>0$ ($2<i<N-1$), $m_{N-1}<0$ and $m_N>0$. At $T_{L,3}=0.7J$, we obtain a one layer transition in which $m_1>0$, $m_2<0$, $m_3<0$, $m_i>0$ ($3<i<N-2$), $m_{N-1}<0$ and $m_N>0$. This transition is a first order wetting phase transition. Indeed, the layer magnetization m_3 (m_{N-2}) becomes discontinuous through the surface transition [42]. As the temperature increases, the wetting transitions of the other layers may occur. All these transitions are first order i. e. the magnetizations m_i ($3<i<N-2$) have the same behaviors as m_3. We remark that these wetting transition temperatures $T_{L,i}$ ($3<i<N-2$) are independent of J_1/J. This is due to strong coupling of J_1 ($|J_1|>J$) and $J_S=1.5J$.

In the second case ($J_1/J\geq -2.5$) the system presents two wetting transition temperatures. The first one is that studied in the case $J_1/J\leq -2.5$. It's followed by another first order wetting transition at a temperature higher than that given in the first wetting transition. This transition point separate the phases ($m_1<0$, $m_2<0$, $m_i<0$ ($2<i<N-1$), $m_{N-1}<0$, $m_N>0$) and $m_1<0$, $m_i>0$ ($1<i<N$), $m_N<0$.

On the other hand, wetting phenomena can not be observed in the amorphized thin film. For example, if we take the fixed value $N=20$, $D/J=-4$, $J_S/J=1.5$, $J_1/J=-4$, $\delta_S=0.5$, the layering transition disappears for $\delta_1\geq 4.94$.

Fig. 10 shows the temperature dependences of each layer, for a crystalline system and when the surafces are coupled antiferromagnetically to the monolayers 2 and ($N-1$). As is seen from Fig. 10a, the first wetting transition temperature T_L^i ($3\leq i\leq 18$) of each layer is observed. In fact, at T_L^i the magnetization m_i exhibits a jump from a positive value to a negative one. Also we remark that at each T_L^i the following layer m_{i+1} presents a small positive jump before its layering transition T_L^{i+1}. In Fig. 10b, the critical temperature of the thin film is given by $T_c^S=T_c^b$. Before this tempearature, two first order wetting transition tempeartures occur for layers 3 and 4. Thus, the first jumps of layers 3 and 4 are analogous of these given in Fig. 10a. On the other hand, their second jumps can occur at the layering transition temperatures of layer 1 and 2.

C. Spin 5/2 at the surfaces and spin 3/2 in the bulk

It is interesting to investigate whether the reentrant phenomena is possible or not depending on the values of the crystal fields. So we present in Fig. 11, the variation of the critical temperature with the amorphization δ_S. Our results are for $N=20$, a strong exchange integral at the surfaces ($J_S/J=4$) and a weak value of J_1/J ($J_1/J=0.1$). As expected, in the absence of anisotropy ($D_1=D_2=0$, curve a), one can observe a reentrant phenomenon when the fluctuations at the surface become strong enough (i.e. $\delta_S>3.99$). Physically, the reentrant behavior has the origin in the competition between ferromagnetic ($J_{ij}>0$) and antiferromagnetic ($J_{ij}<0$) exchange interactions that appear at the surface. However, for δ_S greater than 4.8 the transition temperature of the system converges to the value $4K_Bt_c/J=5.073$. Moreover, for $D_1=0$ and $D_2=-4$ (curve b) the reentrant phenomenon is also observed, but the existence of anisotropy term in the bulk ($D_2\neq 0$) and the increase of the amorphization at the surfaces, give rise to the decrease of the transition temperature of the system until it disappears. Moreover, for $D_1=-4$ and $D_2=0$ (curve c), the reentrant behavior disappears; in fact, the large value of $|D_1|$ cancels the effect of amorphization at the surface.

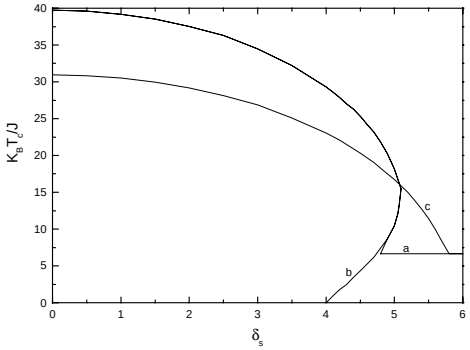

Fig. 11: The phase diagram in the space ($K_B T_c/J, \delta_S$) for several values of anisotropy terms, *N=20*, $J_S/J=4$, $J_1/J=0.1$. $D_1/J=D_2/J=0$ (curve a), $D_1/J=0$, $D_2/J=-4$ (curve b) and $D_1/J=-4$, $D_2/J=0$ (curve c).

IV. CONCLUSION

We have studied the phase diagrams and magnetic properties of a film. Our investigation has revealed many interesting phenomena related to the effects of amorphization and anisotropy surfaces on transition temperature. In the case where there is a spin-1/2 at the surfaces and in the bulk, a 'special point', which exist for *N>3*, move significantly with the amorphization. Furthermore, in the antiferromagnetic case ($J_1 < 0$) wetting phenomena appear. The compensation point is also present when the total magnetization vanishes. In the case where the bulk (spin 1/2) is limited by two surfaces with spin 1, and the surfaces are coupled antiferromagnetically to the bulk, the first order wetting transition T_L^i of each layer i is observed. The wetting phenomenon vanishes with the insertion of strong amorphization. However, when we are dealing with high values of the spin i.e. spin 5/2 at the surfaces and spin 3/2 in the bulk, it is found that for strong amorphization at the surface, a reentrant behavior can appear in the absence of anisotropy terms ($D_1=D_2=0$). However, it should be noted that reentrant behavior is also been predicted to occur when $D_1=0$ and $D_2=-4$.

ACKOWLEDGMENTS

This work was supported by the program PARS Physique 035.

[1] N. M. Jennet and D. J. Dingley, J. Magn. Magn. Mater. **93**, 472 (1991).
[2] A. S. Edelstein, C. Kim, S. B. Qadri, K. H. Kim, V. Browning, H. Y. Yu, B. Maruyama and R. K. Elverett, Solid State Commun. **76**, 1379 (1990).
[3] R. Krishnan, H. O. Gupta, H. Lassri, C. Sella and Kaaboutchi, J. Appl. Phys. **70**, 6421 (1991).
[4] E. Colombo, O. Donzelli, G. B. Fraatucello and F. Ronconi, J. Magn. Magn. Mater **107**, 1857 (1992).
[5] T. Kaneyoshi, I. Tamura, and E. F. Sarmento, Phys. Rev. B **28**,6491 (1983).
[6] C. Tsallis, E. F. Sarmento, and E. L. Albuquerque, J. Magn. Magn. Mater **54**, 667 (1986).
[7] T. Kaneyoshi and T. Balcerzak, Physica A **197**, 667 (1993).
[8] M Jascur and I Kaneyoshi, Phys. Stat. Sol (b) **192**,167 (1995).
[9] T. Kaneyoshi, Phys. Rev. B **39**, 557 (1989).
[10] T. Balcerzak, J. Magn. Magn. Mater **129**, 279 (1994)
[11] M. Bengrine, A. Benyoussef, A. El Kenz, M. Loulidi and F. Mhirech, J. Magn. Magn. Mater **183**, 334 (1998).
[12] M. Bengrine, A. Benyoussef, A. El Kenz, F. Mhirech and L Peliti, submitted to Physica B (1999).
[13] A. R. Ferchmin and W. Maciejewski, J. Phys. C **12**, 4311 (1979).
[14] M. E. Fisher and H. Nakanishi, J. Chem. Phys. **75**, 5857 (1981).
[15] T. Hai and Z. Y. Li, Phys. Stat. Sol. (b) **156**, 641 (1989).
[16] M. Bengrine, A. Benyoussef, A. El Kenz, M. Loulidi and F. Mhirech, Phys. Stat. Sol. (b).**208**, 207 (1998).
[17] M. Bengrine, A. Benyoussef, A. El Kenz, M. Loulidi and F. Mhirech, Physica Scripta **59**, 162 (1999).
[18] M. Bengrine, A. Benyoussef, A. El Kenz, M. Loulidi and F. Mhirech,to be appeared in J. Magn. Magn. Mater. (1999).
[19] R. Honmura and T. Kaneyoshi, J. Phys. C **12**, 3979 (1979).
[20] K. Handrich, Phys. Status. Solidi (b) **32**,K55 (1969).
[21] H. B. Callen, Phys. Lett. **4**, 161 (1963).
[22] T. Kaneyoshi, J. W. Tucker and M. Jascur, Physica A **186**, 495 (1992).
[23] J. C. Cressoni, J. W. Tucker and E. F. Sarmento, J. Appl. Phys. **75**, 10 (1994).
[24] D. Weller, S. F. Alvarado, W. Gudat, K. Schroder, and M. Campagna, Phys. Rev. Lett. **54**, 1555 (1985).
[25] C. Rau, C. Jin and M. Robert, Phys. letters A **138**, 334 (1989).
[26] Y. Jian, Solid State Commun. **74**, 1221 (1990). [27] R. Pandit, M. Schick and M. Wottis, Phys. Rev. B **26**, 8115 (1982)
[28] C. Ebner, C. Rottman and M. Wortis, Phys. Rev. B **28**, 4186 (1983)
[29] C. Ebner and W. F. Saam, Phys. Rev. Lett. **58**, 587 (1987).
[30] C. Ebner, W. F. Saam, Phys. Rev. B **35**, 1822 (1987)
[31] C. Ebner and W. F. Saam and A. K; Sen, Phys. Rev. B. **32**, 1558 (1985).

[32] S. Ramesh and J. D. Maynard, Phys. Rev. lett. **49**, 47 (1982).
[33] S. Ramesh, Q. Zhang, G. Torso and J. D. Maynard, Phys. Rev. lett. **52**, 2375 (1984).
[34] M. Sutton, S. G. J. Mochrie and R. J. Birgeneou, Phys. Rev. lett. **51**, 407 (1983).
[35] S. K. Satija, L. Passel, J. Eckart, W. Ellenson and H. Patterson, Phys. Rev. lett. 51, 411 (1983).
[36] K. Binder and D. P. Landau, Phys. Rev. B 37, 1745 (1988).
[37] A. Patrykiejew, D. P. Landau and K. Binder, Surface Sc. 238, 317 (1990).
[38] A. Benyoussef and H. Ez-zahraouy, J. Phys. I France 4, 393 (1994).
[39] A. Benyoussef and H. Ez-zahraouy, Physica A 206, 196 (1994).
[40] A. Benyoussef and A. El Kenz, Phys. Rev. B **47**, 2619 (1993)
[41] A. Benyoussef, Y. El Amraoui, A. El Kenz and T. Kaneyoshi, Phys. Rev. B **49**, 3920(1994)
[42] L. E. Klebanoff, S. W. Robey, G. Liu and D. A. Shirley, Phys. Rev. B **30**,1048 (1984).